Informes de la Construcción
Vol. 75, 570, e497
abril-junio 2023
ISSN-L: 0020-0883
https://doi.org/10.3989/ic.93713

Optimization and design of the placement of infill walls in 4- and 8-storey structural frames

Optimización y diseño de colocación de muros de relleno en marcos estructurales de 4 y 8 plantas

David J. Domínguez-Santos (*)

ABSTRACT

In construction, brick and concrete are the most widely used materials, occupying an important part of the building budget. Its great versatility in construction, contrasts with the fragility of these elements. This solution is suitable for low-rise buildings, but it is not so clear for medium and high-rise buildings, due to its low ductility and its weight. The proper location of these walls in buildings could improve their resistant and ductile behavior. In this research, the optimal solution is found for the placement of infill walls with bricks in 4- and 8-story frames, considering ductility and resistance.

Keywords: seismic-resistant behavior; brick walls; structures; concrete; frames; push-over analysis.

RESUMEN

En la construcción, el ladrillo y el hormigón son los materiales más utilizados, ocupando una parte importante del presupuesto de edificación. Su gran versatilidad en la construcción contrasta con la fragilidad de estos elementos. Esta solución es adecuada para edificios de baja altura, pero no está tan clara para edificios de altura media y alta, debido a su baja ductilidad y su peso. La correcta ubicación de estos muros en los edificios podría mejorar su comportamiento resistente y dúctil. En esta investigación se encontrará la solución óptima para la colocación de muros de relleno con ladrillos en pórticos de 4 y 8 pisos, considerando ductilidad y resistencia.

Palabras clave: comportamiento sismorresistente; muros de ladrillo; estructuras; hormigón; pórticos; análisis push-over.

(*) Department of Engineering and Building Management, University of Talca, Curicó. (Chile).
Persona de contacto/*Corresponding author*: ddominguez@utalca.cl (David J. Domínguez Santos)
ORCID: https://orcid.org/0000-0001-6664-9011 (D.J. Domínguez Santos)

Cómo citar este artículo/*Citation:* David J. Domínguez-Santos (2023). Optimization and design of the placement of infill walls in 4- and 8-storey structural frames. *Informes de la Construcción,* 75(570): e497. https://doi.org/10.3989/ic.93713

Recibido/*Received*: 04/03/2022
Aceptado/*Accepted*: 13/02/2023
Publicado on-line/*Published on-line*: 13/06/2023

1. INTRODUCTION

Infill walls have demonstrated their structural effectiveness over the years, being the most widely used structural solution in the countries, due to the technical characteristics that these elements produce on buildings (1). In addition, the use of enclosure and partition elements in buildings does not affect the economic section of the same, as they are elements of (almost) mandatory use in buildings. On the other hand, the preference for more solid and durable solutions on the walls (2) of the users, makes it a constructive solution that is highly accepted by people for their houses, regardless of the cost of these. The characteristics provided by this constructive solution, has demonstrated its effectiveness to natural events such as earthquakes produced in seismic countries such as Haiti, Chile, and Japan (3).

Even so, the seismic vulnerability of buildings in countries with low or moderate magnitude earthquakes (4) in recent years, show that the way it is built, and the materials used in construction are not perfect (5-9). For example, (10) reported extensive in-plane and out-of-plane damage to masonry infills in reinforced concrete buildings during the 2009 L'Aquila earthquake. Significant non-structural damage was also observed following the 2010 New Zealand (11) and 2012 Emilia earthquake (12) also in 2016 in central Italy (13). That is why alternatives should be sought to improve the constructive characteristics of buildings.

According to studies carried out, the use of infill walls in buildings improves structural behavior, but, on the contrary, the weight and excessive stiffness that these elements provide to structures affects their earthquake-resistant behavior (14). This has also been confirmed experimentally during laboratory tests performed on the shaking table (15, 16). The numerical comparisons carried out in this investigation have been carried out using the Seismostruct structural program. To solve this without affecting the architectural design and the materials used, this research will delve into the optimization of the number and position of these elements in buildings.

The use of infill walls in low-rise buildings (17, 18) has been shown to improve the seismic and structural behavior of buildings, making them more resistant and rigid. However, in medium and high-rise buildings, due to the great rigidity and weight that these elements contribute to the structures (19-21), it does not make it so relevant. To solve this problem, it has been proposed to replace these elements with other more complex devices: dissipators and base insulators, among others (22-24). Unfortunately, the incorporation of high-tech devices in all types of buildings (especially in low-rise buildings, such as single-family homes) is not viable in society (25-29), due to its cost and the high preparation required for its installation by workers. That is why brick walls (filler) are the most used construction element today to improve the structural performance of buildings, due to the versatility that these elements have in construction.

In many non-seismic countries, such as in seismic countries such as Turkey, Nepal, or Peru (30-32), fired clay bricks used in the walls are still the most widespread solution. Furthermore, in highly seismic countries like Chile, where single-height houses represent 60% of all constructions, most of them are made with fired clay brick walls (43% of the surface of the walls), according to the National Institute of Statistics (INE, 2021) (33) and the Chilean Chamber of Construction (CCHC, 2021) (34).

These elements so widely used in construction have led many researchers to be interested in solving this problem, generating work and research to optimize the use of these construction elements. Examples are the placement of steel sheet walls (35) and infill walls (36), as well as the evaluation of the structural behavior of buildings with these elements (37). The main contribution of this work is to study the optimization of the layout of the infill walls in the different spans that make up the frames. For this, the resistant and ductile behavior of the structures will be studied, important characteristics that are considered in the structural and earthquake resistant behavior.

2. BACKGROUND

The use of infill walls (masonry) in constructions represents a significant percentage of building budgets, reaching up to 30% of it (38).

Clay bricks have been used frequently by many countries in structural (39-41) and non-structural enclosures and in partition walls due to their low cost and good construction characteristics. For this reason, numerous researchers have studied the influence of different additives to the chemical composition of these elements on their thermal (42, 43), acoustic (44) and mechanical (45) properties to improve the structural properties and energy efficiency of buildings. Among such materials, examples are the addition of metallic or polypropylene fibers to the mixture to increase the properties of load capacity (46-48), resistance to shear stress or ductility (49). Likewise, but from an environmental point of view (limiting the damage caused by the extraction of raw materials and/or CO_2 emissions), some mixtures have considered the addition of volcanic ash (50), wood (51), and recycled concrete (52-54), among others.

This type of solution is effective in low-rise and new construction but could be limited in existing and taller buildings. For this, the introduction of stiffeners (braces) (55, 56) and more complex anti-seismic devices such as isolators (57-59) and dissipators (60-62) could be the solution, but the high economic and architectural design cost of this type of solution could also limit their application, especially in buildings for social use.

There are frame structural investigations, where the introduction of brick walls significantly increases the resistance and initial stiffness of constructions (1, 63, 64). These works show the increase in the basal shear and the seismic forces of the buildings when filling walls are incorporated. The initial resistant capacity and stiffness of the buildings is due to the infill walls, so that when this fail, the buildings immediately lose much of their resistance abruptly, continuing the structural behavior that bare buildings would have (only columns and beams) (64).

The good performance of these elements in low-rise frame buildings has made many researchers interested in their behavior (36). Among all the existing solutions, this study delves into the effect that these elements have on structures, considering their layout in plan and elevation. To do this, the structural behavior of these elements in a medium and low-rise building is analyzed, considering the optimal placement that these elements would have in arcaded structures.

3. STRUCTURAL ANALYSIS

This section describes the structural behavior of 4- and 8-storey frame models using nonlinear static analysis (push-over). The calculations were implemented with the structural analysis software Seismostruct v.7.0.2 (2015). This software is based on a finite element analysis, a product of the company Seismosoft® (2015) (65) and allows an estimation of the relationship between the displacement on the top floor and the maximum total base shear of the buildings under static and dynamic loads, considering the behavior of non-linear materials in all their geometries. The results of these non-linear static analysis (push-over) (NLSA) are shown in the respective capacity curves

3.1. Description of the analysed frames

The structures analyzed are frame constructions, due to the use of this structural system in many Latin American and European countries (63, 66) and the ease of inserting infill walls between the columns of frames. These structures are characterized by fast execution times and few material resources. Both aspects are directly related to the reduction of construction costs.

It has been shown in research that the structural behavior of bare frames buildings (beams and columns) (without walls, braces, among others) designed with gravitational loads, is not effective (1, 63, 64) against seismic movements, due to its low resistance. On the other hand, the structural requirements that bare frame buildings designed with seismic-resistant regulations would have in places with medium and high seismicity, make compliance very difficult, without the help of other elements (walls, bracing, among others). Consequently, it is advisable to incorporate structural (shear walls) and non-structural (infill walls) walls to mitigate the possible damage caused (63, 67), complying with the normative requirements.

In recent years, most European countries have been adapting their national (structural) codes to resemble European codes (Eurocodes). For this reason, this work has considered the earthquake resistance Eurocode 8 (EC-8) (EN, 2004) (68) for the design of building models. The elements that make up the frames (beams and columns) have been designed considering the European standard for reinforced concrete (EC-2) and the Spanish standard EHE-08. In these calculations, given the high lateral flexibility of the frames, second-order effects have been considered; however, in most cases the differences with first order analyzes are small. In addition, the calculations have considered the seismic forces obtained from EC-8, for a soil acceleration a_g = 0.20g and a hard soil (type B). Consequently, the results of this work can be considered representative for a significant percentage of existing buildings in Europe and part of Latin America.

The materials used for the structural elements (beams and columns) were concrete HA-30 corresponding to a characteristic resistance of f_{ck} = 300 kg/cm² and steel B-500-S, with an elastic limit of the steel f_{yk} = 5,000 kg/cm2. Both materials are defined in the CTE DB SE AE Standard (2006) (69).

The loads considered in the structural analysis follow the combination of actions G + 0.3Q of Eurocode 8 (2004) (68), where G determines the weight of the structure and Q the live loads (load of use of the building), considering a residential use, administrative or small business, equivalent to 2 kN/m² (2006) (69) in all the floors of the frame except for the upper floor (roof), whose load was 1 kN/m². The surface loads of the slabs have been transferred to the beams of the frames, multiplying them by the length corresponding to the length supported on it.

The present work did not consider the collaboration of the window carpentry in the frame openings due to its great fragility and low resistance. Said space is determined in the empty bays.

Finally, in all the floors of the frame, a rigid diaphragm has been considered corresponding to the effect caused by the 12 cm concrete slab on the structures, an element that limits possible displacements in the vertical axis.

As shown in Figures 1a and 1b, each frame model is made up of 4 spans of 5 meters in length (this measurement is on the column axes). The height between floors is 3 meters, with a free height per floor of 2.60 meters. The horizontal structural elements of the frames correspond to beams 30 cm wide and 40 cm high for all heights. The vertical elements of each frame are made up of five columns of different sizes that vary by 10 cm on each 3 floors. The three upper floors of both models correspond to 30x30 cm columns. The dimensioning of the columns and the beams is detailed in Figures 1a and 1b. The structural continuity of the structural elements is achieved through the longitudinal reinforcements (the steel reinforcement in the concrete that connect the beams and columns), complying with all the requirements of the European codes of structural design.

The total height of the frames is 12 and 24 meters for the 4- and 8-storey buildings, respectively. The configuration of the structures is regular and symmetrical in elevation (Figures 1a and 1b). In the different configurations of the 4- and 8-storey models used, except for the bare frames (case 4_NW and 8_NW), half of the spans are made up of infill walls and the other half are empty, as shown in Figures 2 and 3. The empty openings correspond to the window and door openings that the buildings would have.

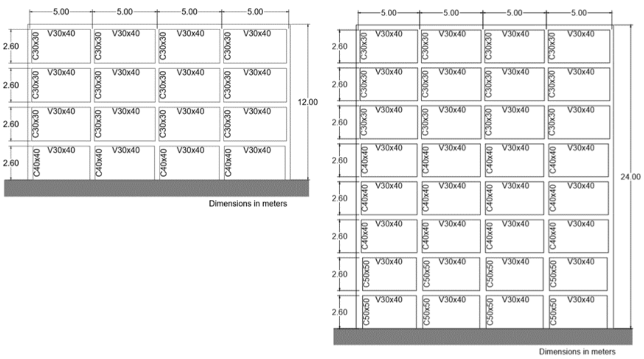

(a) 4-storey frame (b) 8-storey frame

Figure 1. Elevation frames of buildings.

Figures 2 and 3 show the different frame configurations analyzed in this study. The identification of each case is done by means of two terms; a first number that indicates the number of heights of the frames, an underscore (_) and the letter "W" accompanied by another number that indicates the number of the case to which it refers. For example, 4_W6 would be identified with a 4-height frame, being the configuration number 6 of the image corresponding to Figure 2. The case in which the second of the terms is "NW" corresponds to the frames without walls, in the other cases, "Wn" corresponds to the different cases with walls, where "n" is the case number.

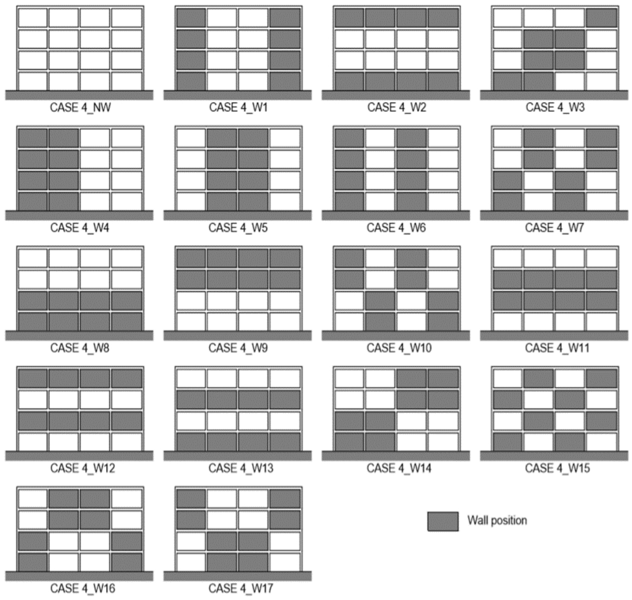

Figure 2. External frames of buildings: 4-storey frame.

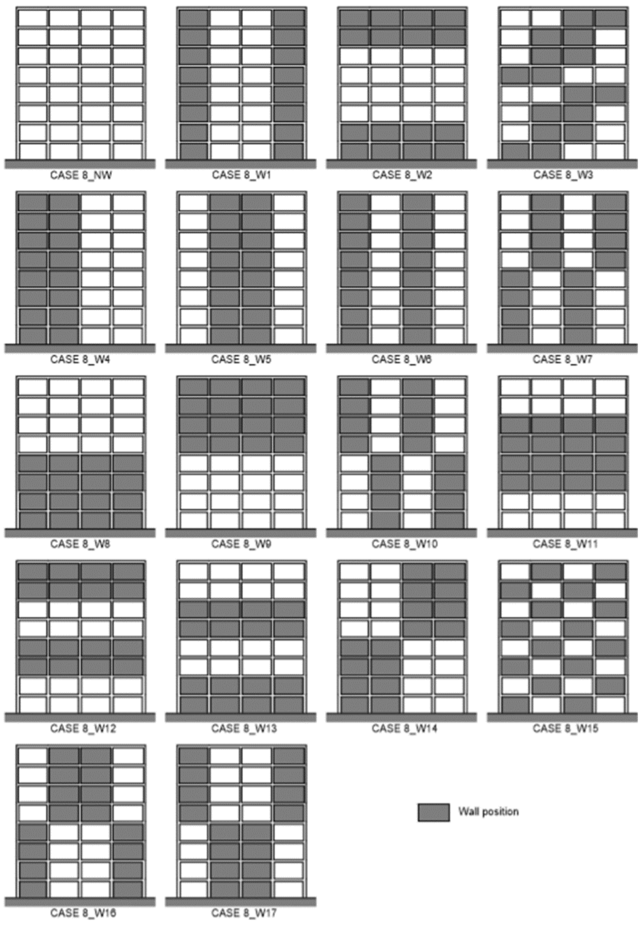

Figure 3. External frames of buildings: 8-storey frame.

The bricks that make up the infill walls of the frames are located under the upper beam of each story without any type of anchoring to the structural elements. These non-structural walls are made up of 23 cm x 12 cm x 10 cm bricks, separated by 1 cm thick mortar with ladder-type steel transverse reinforcements every four rows of bricks, as shown in Figure 4.

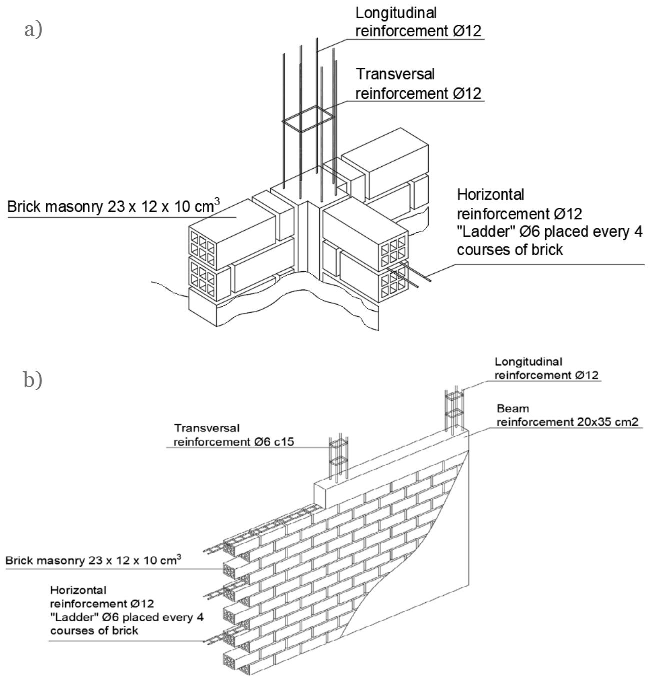

Figure 4. Arrangement of bricks: (a) assembly I; (b) assembly II.

3.2. Main frame modelling

The elements that make up each of the frames were modelled using finite bar elements (70, 71) made up of 2 nodes. For each structural element (columns and beams), its mechanical properties were individually specified following the prescriptions proposed by Mander et al. (1988), for concrete (72) and Ferrara's bilinear model (73) for reinforced steel bars.

In particular, and due to the simplicity and speed of the calculations, the beams and columns that make up the frames are represented by non-linear finite bar elements (74), where the non-linearities are concentrated in the plastic hinges located at the ends, corresponding to 15% of the total length of the element (75, 76). Furthermore, according to Scott et al. (75), it was considered that the joints/connections between the columns and the concrete beams were rigid assuming that the reinforcements used are satisfactorily anchored (connectivity) between the structural elements (beams and columns), while the hysteretic behavior that represents the stress distribution was calculated with fiber models based on the properties of the material and the cross-section of the structural elements (discretized with 300 fibers). In the model, the gravitational loads are applied on the beams, and the horizontal load increment to carry out the non-linear incremental static calculations (push-over), applied laterally on the nodes corresponding to each of the frame heights, follows a triangular loading pattern.

 Informes de la Construcción, Vol. 75, 570, e497, abril-junio 2023. ISSN-L: 0020-0883. https://doi.org/10.3989/ic.93713

The structural analyzes carried out have been considered for a damping of 5%, specified by most of the earthquake resistant Standards (EC-8, NCSE-02, NSR-10, among others) and existing studies.

The simulation of the mechanical behavior of each of the materials that make up the elements of the frame (concrete, steel, and ceramic bricks) requires the entry of various data corresponding to the properties of the material and the requirements established by FEMA and ASCE in relation to the hysterical behavior of the elements that make up the frame were considered sufficient. For this reason, the experimental plasticization and rotation values obtained from the capacity curves of the materials and the structural elements (beams and columns) that make up the frames were considered sufficient. The characteristics of the infill walls are determined in the next section.

3.3. Infill wall modelling

The existence of infill panels modifies the behavior of RC structures. The modelling of the infill wall has been established considering the non-linear inelastic behavior, the determination of the mechanical properties of the materials and the interaction with the frame. In research there are many techniques for analyzing these elements. This work has considered the studies of Crisafulli et al. (76) for computational analysis. To do this, after a detailed review of the different existing analysis, this work adopts the double-strut approach proposed by Crisafulli (77) and implemented by Calvi et al. (78) using Seismosoft® software. The selection of this model has been based on the good results offered by the panel–frame interaction in the modelling and the reasonable computational calculation times. In addition, this type of analysis has been successfully applied for the seismic response of reinforced concrete frames with multi-story infill walls, with verified results (79).

The Crisafulli approach proposes a macro model for the evaluation of the global response of this system. The model is implemented as a four-node panel element, which is connected to the frame at the beam–column joints (Figure 5). Internally, the infill panel element considers the compressive and shear behavior of the masonry panel using two parallel struts and a shear spring in each direction, as indicated in Figures 5a and 5b. This model allows adequate consideration of the lateral stiffness of the panel and the strength of the masonry panel, particularly when shear failure along mortar joints or diagonal stress failure is expected. In the bibliographic reference (79), the numerical analysis on the transformation of the forces in the internal and fictitious nodes into the external forces in the four nodes that make up the panels can be observed in detail.

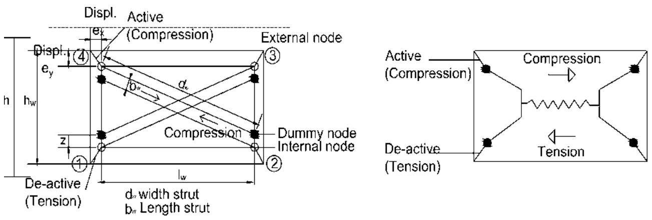

Figure 5. Infill wall model.

For the modelling of the brick elements (infill walls) that make up the masonry panels, a four-node panel element has been considered, developed by the studies carried out by Crisafulli et al. (76). For the modelling of the non-linear response of these panels, the SeismoStruct software has been used, through the studies carried out by Smyrou et al. (80). Each panel is represented by six strut members. Each diagonal direction has two parallel struts to transport axial loads through the two opposite diagonal corners and a third to carry the shear from the top to the bottom of the panel. This last prop only acts through the diagonal that is in compression, so its 'activation' depends on the deformation of the panel. Axial load struts use the masonry strut hysteresis model, while the shear strut uses a bilinear hysteresis structural behavior rule.

Also, as can be observed in Figure 5, four internal nodes are employed to account for the actual points of contact between the frame and the infill panel (i.e. to account for the width and height of the columns and beams, respectively), whilst four dummy nodes are introduced with the objective of accounting for the contact length between the frame and the infill panel. All the internal forces are transformed to the exterior four nodes (which, as noted here, need to be defined in anti-clockwise sequence) where the element is connected to the frame.

The masonry element type is combination of a 3D, force-based, plastic hinge element type employed in modelling mainly the bending behavior of the masonry member (herein referred to as the 'internal sub-element') with two links at the two edges that are employed to simulate the shear behavior of the member (herein referred to as the 'external links' or the 'link sub-elements'). The internal sub-element and the external links are connected in series, ensuring equilibrium in bending moment and shear force. The only 'active' degrees-of-freedom of the link sub-elements are the two translational ones in the shear directions (in-plane and out-of-plane), whilst the other four DOFs (axial and 3 rotational) remain perfectly rigid links. Both masonry walls and spandrels can be accurately modelled with such configuration. The shear DOFs of the link sub-elements feature a hysteretic curve that is based on SeismoStruct's built-in MIMK pinched nonlinear curve (Modified Ibarra–Medina–Krawinkler deterioration curve with bilinear hysteretic rules and pinching), according to a phenomenological law that describes the shear behavior of the entire member. Simultaneously, in the internal sub-element the fiber-section modelling allows for a relatively accurate description of the coupled axial-flexural behavior. The sectional stress–strain state is obtained through the integration of the nonlinear uniaxial material response of the individual fibers, in which the section has been subdivided, fully accounting for the spread of inelasticity along the member length and across the section depth. The determination of the shear strength of the member is crucial for the model's accuracy, and is automatically carried out by the model, based on the masonry's material properties, the dimensions of the member, and the selected Structural Code. The following expressions are employed for the calculation of the member's shear capacity (it is noted that different equations are employed in the different Standards).

The parameters required for the full definition of the element properties are the following tables (Table 1 and 2):

Table 1. Numerical values for geometric and mechanical parameters obtained in the laboratory (part. 1).

Unit	Typical Values	Ordinary bricks used
Shear strength value (Kg/cm²) ACI 530 - 88	8.3	7.8
Poisson ratio	0.1 – 0.3	0.2
Post-peak stiffness (KPa)	-2.5e+6 - -3.0e+7 KPa	-2.5e+6 KPa
Residual Strength	500 – 50000 KPa	10000 KPa
Specific Weight (KN/m³)	24 KN/m³	16.80 KN/m³
Strain at peak stress E_c	0.002 – 0.0022 (m/m)	0.002 (m/m)
Section fibres	150	300
Elastic Stiffness Reduction, a	1.0	1.0
Total shear Deformation Capacity (%)	0.15	0.15
Post-capping Shear Deformation Capacity (%)	1.50	1.50
Ultimate Shear Deformation Capacity (%)	2.00	2.00
Residual Shear Strenght Ratio	0.30	0.30
Shear Deformation Hardening Ratio	0.001	0.001
Cyclic Deterioration Parameters for Shear Streng/Stiffnes	50	50
Ratio of the force at the start of reloading to the max. deformation	0.20	0.20

Table 2. Numerical values for geometric and mechanical parameters obtained in the laboratory (part. 2).

Curve Properties	Typical values	Ordinary bricks used
Initial Young modulus – E_m	400fmθ - 1000 fmθ (kPa)	1812200 (kPa)
Compressive strength – $f_{m\theta}$	-	38100 (kPa)
Tensile strength – f_t (NTC-18)	-	1000 (kPa)
Strain at maximum stress – ε_m	0.001 - 0.005 (m/m)	0.0012 (m/m)
Ultimate strain – ε_u	-	0.024 (m/m)
Closing strain – ε_{cl}	0 - 0.003 (m/m)	0.004 (m/m)
Strut area reduction strain – $\varepsilon 1$	0.0003 - 0.0008 (m/m)	0.0006 (m/m)
Residual strut area strain – $\varepsilon 2$	0.0006 - 0.016 (m/m)	0.001
Starting unload. stiffness factor – γ_{un}	1.5 - 2.5	1.5
Strain reloading factor – α_{re}	0.2 - 0.4	0.2
Strain inflection factor – α_{ch}	0.1 - 0.7	0.7
Complete unloading strain factor – β_a	1.5 - 2.0	1.5
Stress inflection factor – β_{ch}	0.5 - 0.9	0.9
Zero stress stiffness factor – γ_{plu}		1
Reloading stiffness factor – γ_{pr}		1.5
Plastic unloading stiffness factor – $ex1$		3
Repeated cycle strain factor – $ex2$		1.4
Shear bond strength – τ_o	300 - 600 (kPa) (Hendry, 1990) 100 - 1500 (kPa) (Paulay and Priestley, 1992) 100 - 700 (kPa) (Shrive, 1991)	300 KPa
Friction coefficient – μ (ACI-530-88)	0.1 - 1.2	0.67
Maximum shear strength – τ_{MAX}		678 KPa
Reduction shear factor – α_S	1.4 - 1.65	1.5

4. BUILDINGS PERFORMANCE

The different structural design codes describe different procedures for the seismic analysis of buildings. Among the different analysis, this work considers three types of analysis; the simplified method and the spectral analysis of the EC-8 Standard to obtain the seismic forces and perform the dimensioning of the structural elements (beams and columns of the frames) and the NLSA, which is described below, and which will be used to establish the final conclusions of this work.

For this investigation, the same structural sections and materials will be used throughout the frame. The difference in each case will be in the arrangement of the walls in the openings of the frames. To do this, 17 types of filler wall locations will be compared for each of the 2 analyzed frames (4 and 8 stories), in addition to the bare frames (without walls).

4.1. Non-linear static (push-over) analysis

The nonlinear static analysis of incremental thrust is used to estimate the maximum horizontal capacity (base shear) of a structure, considering the deformation and the frequency content of the dynamic response movement. For the evaluation and calculations carried out, the references used were Antoniou and Pinho (81, 82) and Ferracuti et al. (83).

In carrying out the calculations, the lateral load distribution is not kept constant, but is continually updated during the analysis, in accordance with the modal forms and the participation factors derived from the eigenvalue analysis at each step of the calculation process. This method is multimodal, explaining the softening of the structure, the lengthening of its period and the modification of the inertial forces due to spectral amplification.

The constant updating of the triangular lateral load patterns is carried out according to the modal properties that constantly change the system, which provide better response estimates than conventional methods, especially in cases where there are strength or stiffness irregularities in the structure and/or the highest mode effects, according to Pinho, R.et al. (84).

The adaptive algorithm that SeismoStruct implements is very flexible and can accept several different parameters that adapt to the specific requirements of each project. Examples are the SRSS and CQC modal combination methods (Clough and Penzien (85); Chopra (86)).

Non-linear analysis (push-over) allow calculation of the maximum horizontal strength capacity of structures whose dynamic response is not significantly affected by the levels of deformation experienced. That is, the distribution of horizontal forces that simulate the dynamic response can be assumed constant. NLSA is one of four analysis procedures embodied in FEMA 356 (87) and ASCE 41 (88, 89) and is commonly used in performance-based design approaches. For interested readers, a complete description of the method can be found in (87-89).

The methodology followed in this work concentrates on the failures of the frames in the plastic hinges that appear in the areas near the nodes of each structural element (beams and columns). The analysis was made assuming triangular load distributions. This load pattern is increased proportionally with a factor ($\lambda \cdot p$) until structural instability is reached. Additionally, a response control corresponding to an increase in the top floor nodes displacement is used.

The criteria considered in the deformations and failures in this analysis, corresponding to concrete and steel, use the standard values implemented in Seismostruct (90-94), being; concrete cracking (0.0001), concrete detachment (−0.002), crushing the core concrete (0.006), creep (0.0025) and steel fracture (0.06). In addition, the criteria referring to curvature and rotations were verified through the rotational capacity of Mergos (95), and the shear base capacity established in the Eurocode 8 (EC-8). The tolerances used for the displacements and rotations were of the order of 10-5 in all cases, with a maximum number of 300 iterations.

The maximum displacement capacity is predicted considering geometric non-linearities such as inelasticity of materials. The greater or lesser displacement that the structure has is determined based on the number of plastic hinges that are formed in the structure, until it becomes totally unstable.

The legend corresponding to the capacity curves of Figures 6 and 7 that appear on the right side of the same, corresponds to the cases considered in Figures 2 and 3 of section 3.1

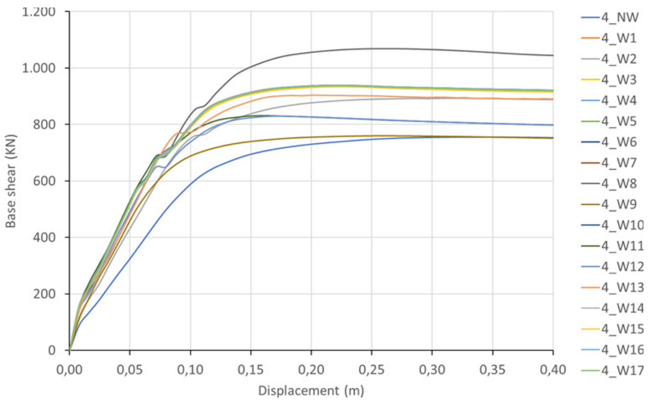

Figure 6. Capacity curves (compression force - deformation) for structural use in 4-storey buildings.

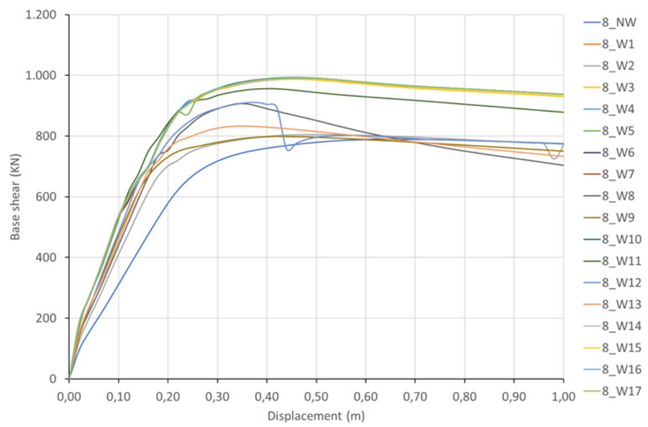

Figure 7. Capacity curves (compression force - deformation) for structural use in 8-storey buildings.

Figures 6 and 7 show the 'non-linear' static behavior of the analyzed 4- and 8-storey models, respectively. The graphs represented allow us to see the elastoplastic behavior of the frames prior to collapse. The beginning of each curve makes it possible to locate the elastoplastic behavior of the structures before the major fault. In the elastic area of the curve (linear part), small differences were observed between the different cases analyzed, except for the bare frames. However, as the applied horizontal force increases, the displacement differences are greater between models for the same load level. During the load increase from 0 kN to the first major failure, it is the infill walls that resist the shear forces applied to the structures. These elements increase the initial stiffness of the structure, causing the main structural elements (beams and columns) to fail later. This is observed with a significant reduction in the structural rigidity of the frames once their maximum strength is reached. On the other hand, it can also be observed how the structural behavior of buildings, once the maximum shear is reached, tends to equalize. This is due to the collapse of the infill walls in the initial part of the graph's capacity curves, the main elements (beams and columns) being those that support the frame structure once the maximum resistance produced by the walls has been reached.

The plasticity in the capacity curves is mainly generated by the cracks produced in the concrete and bricks that make up the infill walls and the plasticity of the existing steel reinforcement in the primary structural elements. These effects are determined by the formation of plastic hinges in each element. The greater or lesser number of hinges that are formed in each case analyzed prior to the collapse will determine the length of these curves and the ductility of the frames.

The structural performance of brick-walled frames generates a significant increase in shear force when compared to the structure without any type of wall. The maximum value reached for both frame structures is between 800 kN and 1000 kN in the case of frames with infill walls, this being approximately 20% higher in most of the cases analyzed than frames without walls. After these failures, a slight decrease in the structural performance of the cases can be observed. The displacement and resistance in the frames with infill walls is associated with the location of the walls in the frames, which generates more ductile structures.

Finally, due to the increased ductility, it is possible to see that the first major failure in most of the 4-storey frames occurs with an approximate displacement of 100 mm in structures with walls, being slightly higher in frames without walls (134 mm). On the other hand, in the 8-storey frames, the first major failure in most of the structures with walls occurs with a displacement of 200 mm, being slightly lower in the frames without walls (269 mm). This proportional relationship of displacements is produced because they are structures with similar stiffnesses.

Table 3 show the values of the ductility, fundamental period, deformation and plastic and ultimate resistance in the frames of 4 and 8 stories. Obviously, the results show greater ductility in frames without walls. The percentages of values included in parentheses in table 2 correspond to the increase in these values with respect to the frames without any walls.

Analysis of the best behaviors ranks cases 4_W8 and 8_W10 as the most resistant and cases 4_W9 and 8_W2 as the most ductile. Similarly, cases 4_NW and 8_NW are the least strong and cases 4_W12 and 8_W8 are the least ductile.

By selecting the 6 most resistant and ductile frames, they confirm that the walls are concentrated in the external openings and in the upper part of them.

Table 3. Deformations base shear and ductility for structural use in 4-storey buildings and 8-storey buildings.

Frame type	Fundamental Period (T) (s)	Plastic deformation (δ_p) (m)	Ultimate deformation (δ_u) (m)	Base Shear Plastic force (kN)	Base Shear Ultimate force (kN)	Ductility ($\mu = \delta_u/\delta_p$)
4_NW (Bare frame)	0.46	0.134	0.356	676	756	2.50
4_W1	0.29 (-37%)	0.102 (-24%)	0.223 (-37%)	816 (+21%)	938 (+24%)	2.19 (-23%)
4_W2	0.30 (-35%)	0.119 (-12%)	0.297 (-17%)	787 (+16%)	893 (+18%)	2.30 (-8%)
4_W3	0.29 (-37%)	0.104 (-23%)	0.224 (-37%)	806 (+19%)	934 (+23%)	2.15 (-14%)
4_W4	0.29 (-37%)	0.103 (-24%)	0.224 (-37%)	813 (+20%)	939 (+24%)	2.16 (-14%)
4_W5	0.29 (-37%)	0.103 (-24%)	0.224 (-37%)	811 (+20%)	938 (+24%)	2.16 (-14%)
4_W6	0.29 (-37%)	0.103 (-24%)	0.224 (-37%)	814 (+20%)	939 (+24%)	2.16 (-14%)
4_W7	0.29 (-37%)	0.104 (-23%)	0.223 (-37%)	810 (+20%)	938 (+24%)	2.15 (-14%)
4_W8	0.27 (-41%)	0.117 (-13%)	0.264 (-26%)	941 (+39%)	1068 (+41%)	2.08 (-17%)
4_W9	0.31 (-33%)	0.112 (-17%)	0.263 (-26%)	678 (+0.3%)	759 (+0.4%)	2.35 (-6%)
4_W10	0.29 (-37%)	0.102 (-24%)	0.224 (-37%)	816 (+21%)	938 (+24%)	2.18 (-13%)
4_W11	0.28 (-39%)	0.083 (-38%)	0.160 (-55%)	692 (+2%)	831 (+10%)	1.93 (-23%)
4_W12	0.30 (-35%)	0.092 (-32%)	0.175 (-51%)	724 (+7%)	830 (+10%)	1.91 (-23%)
4_W13	0.27 (-41%)	0.102 (-24%)	0.200 (-44%)	779 (+15%)	904 (+19%)	1.96 (-22%)
4_W14	0.29 (-37%)	0.105 (-22%)	0.223 (-37%)	807 (+19%)	938 (+24%)	2.13 (-15%)
4_W15	0.29 (-37%)	0.103 (-24%)	0.224 (-37%)	810 (+20%)	934 (+23%)	2.17 (-13%)
4_W16	0.29 (-37%)	0.103 (-24%)	0.224 (-37%)	813 (+20%)	939 (+24%)	2.17 (-13%)
4_W17	0.28 (-39%)	0.103 (-24%)	0.224 (-37%)	812 (+20%)	938 (+24%)	2.17 (-13%)
8_NW (Bare frame)	0.91	0.269	0.640	701	789	2.38
8_W1	0.79 (-13%)	0.217 (-20%)	0.460 (-28%)	880 (+26%)	992 (+26%)	2.12 (-11%)
8_W2	0.83 (-9%)	0.220 (-19%)	0.500 (-22%)	719 (+3%)	804 (+2%)	2.27 (-5%)
8_W3	0.79 (-13%)	0.217 (-20%)	0.460 (-28%)	874 (+25%)	987 (+25%)	2.12 (-11%)
8_W4	0.80 (-12%)	0.218 (-20%)	0.460 (-28%)	878 (+25%)	992 (+26%)	2.11 (-11%)
8_W5	0.79 (-13%)	0.220 (-19%)	0.460 (-28%)	878 (+25%)	992 (+26%)	2.09 (-12%)
8_W6	0.79 (-13%)	0.217 (-20%)	0.460 (-28%)	880 (+26%)	992 (+26%)	2.11 (-11%)
8_W7	0.79 (-13%)	0.219 (-20%)	0.460 (-28%)	877 (+25%)	990 (+25%)	2.10 (-12%)
8_W8	0.72 (-21%)	0.220 (-20%)	0.340 (-47%)	801 (+14%)	907 (+15%)	1.54 (-35%)
8_W9	0.86 (-6%)	0.185 (-32%)	0.407 (-36%)	705 (+0.6%)	799 (+1%)	2.19 (-8%)
8_W10	0.79 (-13%)	0.217 (-20%)	0.460 (-28%)	881 (+26%)	993 (+26%)	2.12 (-11%)
8_W11	0.75 (-18%)	0.200 (-26%)	0.400 (-37%)	842 (+20%)	956 (+21%)	2.00 (-16%)
8_W12	0.84 (-8%)	0.207 (-23%)	0.380 (-41%)	781 (+11%)	910 (+15%)	1.83 (-23%)
8_W13	0.75 (-18%)	0.190 (-30%)	0.340 (-47%)	759 (+8%)	833 (+6%)	1.79 (-25%)
8_W14	0.79 (-13%)	0.218 (-20%)	0.460 (-28%)	874 (+25%)	989 (+25%)	2.10 (-12%)
8_W15	0.79 (-13%)	0.217 (-20%)	0.460 (-28%)	878 (+25%)	990 (+25%)	2.11 (-11%)
8_W16	0.79 (-13%)	0.217 (-20%)	0.460 (-28%)	879 (+25%)	992 (+26%)	2.11 (-11%)
8_W17	0.79 (-13%)	0.217 (-20%)	0.460 (-28%)	878 (+25%)	992 (+26%)	2.11 (-11%)

5. DISCUSSION

The bricks used in walls have achieved a wide diffusion in construction due to their remarkable resistance, thermal and acoustic insulation, fire resistance and low moisture absorption. However, seismic countries like Chile, Japan and many others also require materials with good earthquake resistant behavior.

Among the construction solutions that improve the earthquake-resistant behavior of buildings is the reduction of the weight of the buildings, the increase in ductility and the inclusion of anti-seismic devices such as dissipators, isolators, bracing and the inclusion of infill walls in the buildings, devices that are necessary for regulatory compliance in seismic countries such as Chile.

In general, the introduction of walls in buildings is beneficial for structures, but nevertheless increases the weight and fragility of buildings. That is why finding more ductile and resistant solutions using the same materials is important in the world of construction.

Placing ordinary infill walls in the 4- and 8-storey frames improves by up to 41% (4_W8) and 26% (8_W10) respectively the resistance of the frames without walls.

The cases of frames without walls (4_NW and 8_NW) have greater ductility, due to the greater displacement and less fragility that the frames have as there are no walls. In these cases, the formation of plastic hinges occurs more slowly in the primary structural elements (columns and beams) than in the cases with walls. The increase in strength and rigidity of the frames is due to the introduction of infill walls, which are those that resist the structure, once they collapse, the damage is transferred to the structural elements (beams and columns), producing failures more fragile.

The inclusion of infill walls improves the resistant behavior of bare frames; however, its ductility is reduced. The location of the walls in certain spans could improve up to 41% and 26% the strength of bare 4-storey and 8-storey frames respectively.

On the other hand, although the placement of walls reduces the ductility of the bare frames, their location between the spans significantly affects, improving up to 15% and 47% the frames with walls of 4 and 8 storey respectively.

Figures 8 and 9 show a relationship of the basal shear and ductility in the different analyzed frames of 4 and 8 stories, respectively. The dotted line LT shows the mean trend curve that relates shear to ductility. In the 8-storey frames, the cases analyzed have more dispersed results around the trend line. In both figures, case concentrations are shown around similar ductility and basal shear. In the 4-storey frames, a concentration of ductility cases is shown around 2.15 and basal shear around 950 kN, while in the 8-storey frames a concentration of ductility cases is shown around 2.1 and basal shear around 1000 kN.

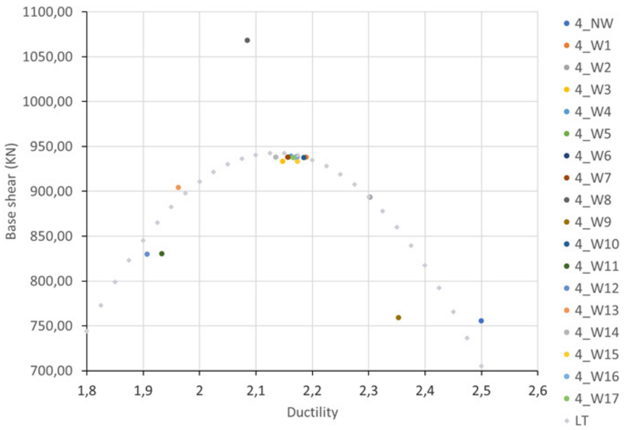

Figure 8. Basal shear–ductility and trend curve in 4-storey buildings.

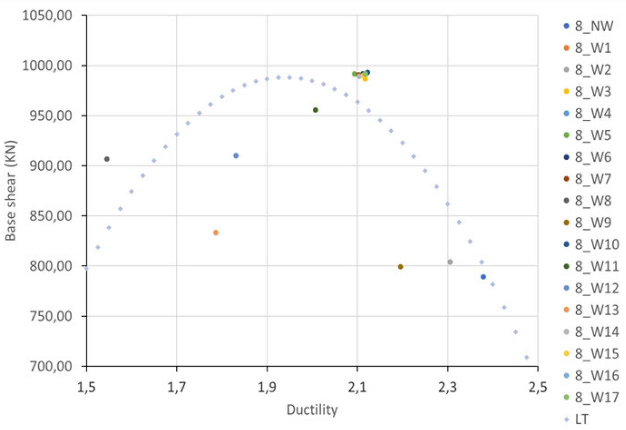

Figure 9. Basal shear–ductility and trend curve in 8-storey buildings.

6. CONCLUSIONS

This work analysis the structural behavior of frames of 4 and 8 stories, changing the arrangement of the walls between the openings that compose it. In this investigation, two frames of 4 and 8 heights have been used with a regular configuration in elevation, with the same type of rectangular beams on all stories high and square columns on all heights, varying their dimensions every 3 heights by 10 cm on each axis. The connection of beams and columns is rigid. On the other hand, the walls used are made of perforated ceramic bricks of 23 x 12 x 10 cm^3, not being anchored to the main structure. The great rigidity infringed by the bricks in the walls is solved by including longitudinal reinforcements every four rows of these elements, anchored to the longitudinal reinforcement of the columns. The work methodology included the realization of NLSA and comparative statistics of the different cases analyzed, considering their ductility and resistance. The following conclusions can be drawn from the results:

- The inclusion of infill walls significantly increases the resistance of the frames. The best cases correspond to those wall locations that do not leave any row or column of empty openings.
- The initial structural behavior (stiffness and resistance) of the capacity curves of the frames is due to the infill walls. Once they have failed, the curves descend tending to continue the structural behavior of the bare frames.
- The most ductile frames analyzed correspond to bare frames. In the case of infill walls, the most ductile cases correspond to frames with walls concentrated on the upper floors of the same. In addition, the most ductile cases are those that lack walls on the central floors of the frames.
- The most resistant frames analyzed correspond to those that concentrate the infill walls in their outer openings (bays). The most resistant cases correspond to the frames that concentrate the walls on the ground floors in the 4-storey frames, while in the 8-storey frames, the location of the walls occurs with a balanced distribution of the walls on all floors.
- The least resistant structural frames are those that concentrate the infill walls on the upper floors, leaving some floors empty (without walls), especially the floors of the lower floors.
- All the cases studied in this work refer to exterior frames, corresponding to the enclosures of the buildings, being those that would give a greater resistance to the buildings. The interior distributions in this investigation have not been considered, since a greater number of interior partitions would improve the behavior of the buildings, significantly increasing the resistance of the buildings. In this investigation, the most unfavorable building cases have been considered, corresponding to open floors (without any interior partition), not considering the increases in rigidity and resistance exerted by them. On the other hand, considering that the best seismic-resistant solutions correspond to constructions with greater resistance and ductility, it can be affirmed that the best solutions would correspond to frames in which each story has a wall. Considering that there are no optimal solutions with the highest ductility and resistance together, it can be affirmed that the best solutions would correspond to the cases that have a good behavior in both properties. For this, in section 5 "Discussions", some cur-

ves have been established that perfectly determine the best solutions, corresponding to the cases closest to the maximum of the curves represented (Figures 8 and 9). It is concluded that there is no case that significantly improves the others, but that there are several correct solutions. For the 4-height frame, the best solutions would be: 1, 2, 3, 4, 5, 6, 7, 15, and 16 and for the 8-height frame: 2, 3, 5, 6, 7, 10, 11, 15 and 17.

REFERENCES

(1) Domínguez Santos, D.J., López Almansa, F., Benavent Climent, A. (2014). Behavior, for the Lorca earthquake on 11-05-2011, of wide beam building designed without seismic considerations. *Informes de la Construcción*, 66(533). https://doi.org/10.3989/ic.12.092.

(2) Nettleton, S., Martin, D., Buse, C., & Prior, L. (2020). Materializing architecture for social care: Brick walls and compromises in design for later life. *The British journal of sociology*, 71(1), 153-167. https://doi.org/10.1111/1468-4446.12722.

(3) Doocy, S., Daniels, A., Packer, C., Dick, A., Kirsch, T.D. (2013). The human impact of earthquakes: a historical review of events 1980-2009 and systematic literature review. *PLoS currents*, 5. https://doi.org/10.1371/currents.dis.67bd14fe457f1db0b5433a8ee20fb833.

(4) Dominguez-Santos, D., Ballesteros-Perez, P., Mora-Melia, D. (2017). Structural resistance of reinforced concrete buildings in areas of moderate seismicity and assessment of strategies for structural improvement. *Buildings*, 7(4), 89. https://doi.org/10.3390/buildings7040089.

(5) Dominguez D., Muñoz Velasco, P. (2017). Impact of Lightweight fired clay bricks used as enclosures for individual houses of one story on zones of high seismicity. *Materiales de la Construcción*, 67(328), e133. https://doi.org/10.3989/mc.2017.03316.

(6) Dominguez-Santos, D., Mora-Melia D., BallesterosPerez, P., Pincheira- Orellana, G., Retamal-Bravo C. (2019). Study of mechanical properties and seismic performance in wood-concrete composite blocks for building construction. *Materials (Basel).* https://doi.org/10.3390/ma12091500.

(7) Dominguez, D., Letelier, V., Muñoz. P. (2019). Seismic capacity of 2- and 3-storey RC buildings with eco-concrete made by using residues for replacing natural aggregates. *Journal of Building Engineering*. 28, 101086. https://doi.org/10.1016/j.jobe.2019.101086.

(8) Dominguez, D., Pallarés, F., Llanos, P. (2021). Seismic structural performance ofconcrete blocks with steel and aluminum alloy fiber aggregates for building construction. *Mechanics of Advanced Materials and Structures*. https://doi.org/10.1080/15376494.2021.1988190.

(9) Wahid, S.A., Rawi, S. M., Desa, N.M. (2015). Utilization of plastic bottle waste in sand bricks. Journal of Basic and Applied Scientific Research, 5(1), 35-44. ISSN 2090-4304.

(10) Braga, F., Manfredi, V., Masi, A. et al. (2011). Performance of non-structural elements in RC buildings during the L'Aquila, 2009 earthquake. *Bull Earthquake Eng,* 9, 307–324 https://doi.org/10.1007/s10518-010-9205-7.

(11) Dhakal, R.P. (2010). Damage to non-structural components and contents in 2010 Darfield earthquake. *Bulletin of the New Zealand Society for Earthquake Engineering,* 43(4), 404–411. https://doi.org/10.5459/bnzsee.43.4.404-411.

(12) Ercolino, M., Ricci, P., Magliulo, G., Verderame, G.M. (2016). Influence of infill panels on an irregular RC building designed according to seismic codes. *Earthquakes and Structures*, 10(2), 261-291. https://doi.org/10.12989/eas.2016.10.2.261.

(13) Perrone, D., Calvi, P.M., Nascimbene, R., Fischer, E.C., Magliulo, G. (2019). Seismic performance of non-structural elements during the 2016 Central Italy earthquake. *Bulletin of Earthquake Engineering*, 17(10), 5655-5677. https://doi.org/10.1007/s10518-018-0361-5.

(14) López-Almansa, F., Domínguez, D., & Benavent-Climent, A. (2013). Vulnerability analysis of RC buildings with wide beams located in moderate seismicity regions. *Engineering structures*, 46, 687-702. https://doi.org/10.1016/j.engstruct.2012.08.033.

(15) Bianchi, F., Nascimbene, R., & Pavese, A. (2017). Experimental. Numerical simulations: Seismic response of a half scale three-storey infilled RC building strengthened using FRP retrofit. *The Open Civil Engineering Journal*, 11(1). https://doi.org/10.2174/1874149501711011158.

(16) Nascimbene, R. (2015). Numerical model of a reinforced concrete building: Earthquake analysis and experimental validation. *Periodica Polytechnica Civil Engineering*, 59(4), 521-530. https://doi.org/10.3311/PPci.8247.

(17) Avila, L., Vasconcelos, G., Lourenço, P. B., Mendes, N., Alves, P., Costa, A. C. (2012). Seismic response analysis of concrete block masonry buildings: An experimental study using shaking table. http://hdl.handle.net/1822/21832.

(18) Frasson Jr. A., Casali, J.M., Oliveira, A. L., Prudêncio Jr. L.R. (2012, June). A Mix design methodology for concrete block units. In Proceedings of the 15th International Brick and Block Masonry Conference, Florianapolis, Brazil (pp. 3-6).

(19) El Zareef, M.A., El Madawy, M.E. (2018). Optimization of infill panel for seismic response of multi-story RC frame buildings utilizing multi criteria optimization technique. *Bulletin of Earthquake Engineering*, 16(10), 4951-4970. https://doi.org/10.1007/s10518-018-0363-3.

(20) Kumar, B. R., Sandhyarani, D., Scholar, P. (2015). Shear wall analysis and design optimization in case of high rise buildings. *International Journal of Scientific & Engineering Research*, 6(1), 546-559.

(21) Li, J., Chen, L., Wang, X., & Li, F. (2022). *Study and Numerical Analysis on Seismic Performance of Concrete U-Shaped Shear Wall. Advances in Materials Science and Engineering,* 2022. https://doi.org/10.1155/2022/2838691.

(22) Clemente, P., Buffarini, G. (2010). Base isolation: design and optimization criteria. *Seismic Isolation and Protection Systems*, 1(1), 17-40. https://doi.org/10.2140/siaps.2010.1.17.

(23) Marano, G.C., Greco, R., Palombella, G. (2008). *Stochastic optimum design of linear tuned mass dampers for seismic protection of high towers. Structural Engineering and Mechanics,* 29(6), 603-622. https://doi.org/10.12989/sem.2008.29.6.603.

(24) Islam, A.B.M.S., Jameel, M., Jumaat, M.Z., Rahman, M.M. (2013). Optimization in structural altitude for seismic base isolation at medium risk earthquake disaster region. *Disaster Advances,* 6(1), 23-34. https://www.researchgate.net/publication/266895951.
(25) Cocco, G., D'Aloisio, A., Spacone, E., Brando, G. (2019). Seismic vulnerability of buildings in historic centers: from the "urban" to the "aggregate" scale. *Frontiers in Built Environment*, 5, 78. https://doi.org/10.3389/fbuil.2019.00078.
(26) Labo, S., Passoni, C., Marini, A., Belleri, A., Camata, G., Riva, P., Spacone, E. (2016). Diagrid solutions for a sustainable seismic, energy, and architectural upgrade of European RC buildings. In XII International Conference on Structural Repair and Rehabilitation. PT.
(27) Sorace, S., Terenzi, G. (2014). A viable base isolation strategy for the advanced seismic retrofit of an R/C building. *Contemp. Eng. Sci.*, 7(17-20), 817-834. http://doi.org/10.12988/ces.2014.4549.
(28) De Domenico, D., Impollonia, N., Ricciardi, G. (2019). Seismic retrofitting of confined masonry-RC buildings: The case study of the university hall of residence in Messina, Italy. *International Journal of Earthquake Engineering*. 36(1):54-85
(29) Sorace, S., Terenzi, G. (2016). Analysis and seismic isolation of an older reinforced concrete vaulted building. *Contemp. Eng. Sci.*, 9, 1201-1215. http://doi.org/10.12988/ces.2016.66110.
(30) De Landa, M. (1997). A thousand years of nonlinear history. ISBN(s) 0942299329 0942299310.
(31) Mehta, P.K., Monteiro, P J. (2014). Concrete: microstructure, properties, and materials. McGraw-Hill Education. ISBN: 9780071797870.
(32) Thorat, T.S.V.M., Papal, M., Kacha, V., Sarnobat, T., Gaikwad, S. (2015). Hollow concrete blocks-A new trend. *International Journal of Engineering & Research*, 5(5), 9-26. ISSN: 2249–6645.
(33) Instituto Nacional de Estadísticas de Chile (INE) (2021). Ministerio de Economía, Fomento y Turismo. Retrieved form https://www.ine.cl/
(34) CCHC (2021). Cámara de la construcción de Chile. Retrieved form https://cchc.cl/.
(35) Gholizadeh, S., Shahrezaei, A.M. (2015). Optimal placement of steel plate shear walls for steel frames by bat algorithm. *The Structural Design of Tall and Special Buildings*, 24(1), 1-18. https://doi.org/10.1002/tal.1151.
(36) Güney, D., Kuruşçu, A.O. (2011). Optimization of the configuration of infill walls in order to increase seismic resistance of building structures. *Int. J. Phys. Sci.,* 6(4), 698-706. http://www.academicjournals.org/IJPS.
(37) Hashemi, S.A. (2007). Seismic evaluation of reinforced concrete buildings including effects of masonry infill walls. University of California, Berkeley. PEER Report 2007/100.
(38) Generador de Precios (2021). CYPE Ingenieros, S.A. Retrieved form http://www.chile.generadordeprecios.info/.
(39) Domínguez, D., Munoz, V.P., Munoz, V.L. (2017). Impact of using lightweight eco-bricks as enclosures for individual houses of one story on zones of high seismicity. *Materiales de Construcción*, 67(328), e133. https://doi.org/10.3989/mc.2017.03316.
(40) Mir, B.A. (2015). Some studies on the effect of fly ash and lime on physical and mechanical properties of expansive clay. *International Journal of Civil Engineering,* 13(3), 203-212. IJCE 2015, 13(3 And 4B): 203-212.
(41) Domínguez, D., López-Almansa, F., Benavent Climent, A. (2014). Comportamiento, para el terremoto de Lorca de 11-05-2011, de edificios de vigas planas proyectados sin tener en cuenta la acción sísmica. http://doi.org/10.3989/ic.12.092.
(42) Zhu, L., Dai, J., Bai, G., Zhang, F. (2015). Study on thermal properties of recycled aggregate concrete and recycled concrete blocks. *Construction and Building Materials*, 94, 620-628. https://doi.org/10.1016/j.conbuildmat.2015.07.058.
(43) Miličević, I., Bjegović, D., Siddique, R. (2015). Experimental research of concrete floor blocks with crushed bricks and tiles aggregate. *Construction and Building materials,* 94, 775-783. https://doi.org/10.1016/j.conbuildmat.2015.07.163.
(44) Pastor, J.M., García, L.D., Quintana, S., Peña, J. (2014). Glass reinforced concrete panels containing recycled tyres: Evaluation of the acoustic properties of for their use as sound barriers. *Construction and Building Materials*, 54, 541-549. https://doi.org/10.1016/j.conbuildmat.2013.12.040.
(45) Ergün, A. (2011). Effects of the usage of diatomite and waste marble powder as partial replacement of cement on the mechanical properties of concrete. *Construction and building materials*, 25(2), 806-812. https://doi.org/10.1016/j.conbuildmat.2010.07.002.
(46) Mindess, S., Vondran, G. (1988). Properties of concrete reinforced with fibrillated polypropylene fibres under impact loading. *Cement and Concrete Research*, 18(1), 109-115. https://doi.org/10.1016/0008-8846(88)90127-5.
(47) Bayasi, Z., McIntyre, M. (2002). Application of fibrillated polypropylene fibers for restraint of plastic shrinkage cracking in silica fume concrete. *Materials Journal*, 99(4), 337-344. Retrieved from https://www.concrete.org/publications/acimaterialsjournal.aspx
(48) Ashour, S.A., Wafa, F.F. (1993). Flexural behavior of high-strength fiber reinforced concrete beams. *Structural Journal*, 90(3), 279-287. Retrieved from http://www.concrete.org/PUBS/JOURNALS/SJHOME.ASP.
(49) Oh, B.H. (1992). Flexural analysis of reinforced concrete beams containing steel fibers. *Journal of Structural Engineering*, 118(10), 2821-2835. https://doi.org/10.1061/(ASCE)0733-9445(1992)118:10(2821).
(50) Sabir, B.B., Wild, S., Bai, J. (2001). Metakaolin and calcined clays as pozzolans for concrete: a review. *Cement and Concrete Composites,* 23(6), 441-454. https://doi.org/10.1016/S0958-9465(00)00092-5.
(51) Quaranta, N., Caligaris, M., López, H., Unsen, M., Di Rienzo, H. (2008). Adición de aserrines de descarte en la producción de mampuestos cerámicos. In Actas del Octavo Congreso Internacional de Metalurgia y Materiales.
(52) Nili, M., Sasanipour, H., Aslani, F. (2019). The effect of fine and coarse recycled aggregates on fresh and mechanical properties of self-compacting concrete. *Materials*, 12(7), 1120. https://doi.org/10.3390/ma12071120
(53) Xie, J., Zhao, J., Wang, J., Wang, C., Huang, P., Fang, C. (2019). Sulfate resistance of recycled aggregate concrete with GGBS and fly ash-based geopolymer. *Materials*, 12(8), 1247. https://doi.org/10.3390/ma12081247
(54) Liu, W., Cao, W., Zhang, J., Qiao, Q., Ma, H. (2016). Seismic performance of composite shear walls constructed using recycled aggregate concrete and different expandable polystyrene configurations. *Materials*, 9(3), 148. https://doi.org/10.3390/ma9030148.

(55) Ozcelik, R., Dikiciasik, Y., Erdil, E.F. (2017). The development of the buckling restrained braces with new end restrains. *Journal of Constructional Steel Research,* 138, 208-220. https://doi.org/10.1016/j.jcsr.2017.07.008.

(56) Qiao, S., Han, X., & Zhou, K. (2017). Bracing configuration and seismic performance of reinforced concrete frame with brace. *The Structural Design of Tall and Special Buildings*, 26(14), e1381. https://doi.org/10.1002/tal.1381.

(57) Eem, S.H., Jung, H.J., Koo, J.H. (2011). Application of MR elastomers for improving seismic protection of base-isolated structures. *IEEE Transactions on Magnetics*, 47(10), 2901-2904. https://doi.org/10.1109/TMAG.2011.2156771

(58) Tomaževič, M., Klemenc, I., Weiss, P. (2009). Seismic upgrading of old masonry buildings by seismic isolation and CFRP laminates: a shaking-table study of reduced scale models. *Bulletin of Earthquake Engineering*, 7(1), 293-321. https://doi.org/10.1007/s10518-008-9086-1.

(59) Buchanan, A.H., Bull, D., Dhakal, R., MacRae, G., Palermo, A., Pampanin, S. (2011). Base isolation and damage-resistant technologies for improved seismic performance of buildings. Retrieved from http://hdl.handle.net/10092/10218.

(60) Martinez-Romero, E. (1993). Experiences on the use of supplementary energy dissipators on building structures. Earthquake spectra, 9(3), 581-625. https://doi.org/10.1193/1.1585731.

(61) Miyamoto, H.K., Singh, J.P. (2002). Performance of structures with passive energy dissipators. *Earthquake Spectra*, 18(1), 105-119. https://doi.org/10.1193/1.1468650.

(62) Mata, P., Barbat, A.H., Oller, S., Boroschek, R. (2008). Constitutive and geometric nonlinear models for the seismic analysis of RC structures with energy dissipators. *Archives of Computational Methods in Engineering*, 15(4), 489. https://doi.org/10.1007/s11831-008-9024-z.

(63) Domínguez, D., López-Almansa, F., Benavent-Climent, A. (2016). Would RC wide-beam buildings in Spain have survived Lorca earthquake (11-05-2011)?. *Engineering Structures*, 108, 134-154. https://doi.org/10.1016/j.engstruct.2015.11.020.

(64) Domínguez Santos, D.J., López Almansa, F., Benavent Climent, A. (2011). Evaluación del comportamiento sismorresistente de edificios de hormigón con vigas planas. In 4º Congreso nacional de ingeniería sísmica: libro de resumenes: Granada, 18-20 mayo de 2011. Copicentro.

(65) Seismo Soft. A Computer Program for Static and Dynamic Nonlinear Analysis of Framed Structures (2015). Retrieved from http://www.seismosoft.com (accessed on day, month, year).

(66) Gómez-Martínez, F., Alonso-Durá, A., De Luca, F., & Verderame, G.M. (2016). Seismic performances and behaviour factor of wide-beam and deep-beam RC frames. *Engineering Structures*, 125, 107-123. https://doi.org/10.1016/j.engstruct.2016.06.034.

(67) CTE DEB SE F, (Spanish Standard) (2006). Documento Básico. Código Técnico de la Edificación. Seguridad Estructural: Fabrica; Ministerio de Fomento: Madrid, Spain.

(68) EN 1998. Eurocode 8 (2004). Design of structures for earthquake resistance. European Committee for Standarization.

(69) CTE DEB SE AE, (Spanish Standard) (2006). Documento Básico. Código Técnico de la Edificación. Acciones en la edificación; Ministerio de Fomento: Madrid, Spain.

(70) Scott, M.H., Fenves, G.L. (2006). Plastic hinge integration methods for force-based beam–column elements. *Journal of Structural Engineering*, 132(2), 244-252. https://doi.org/10.1061/(ASCE)0733-9445(2006)132:2(244).

(71) Zienkiewicz, O.C., Taylor, R.L. (2000). The finite element method, vol. 2. Butterworth-Heinemann. ISBN 0 7506 5055 9.

(72) Mander, J.B., Priestley, M.J., Park, R. (1988). Theoretical stress-strain model for confined concrete. Journal of structural engineering, 114(8), 1804-1826. https://doi.org/10.1061/(ASCE)0733-9445(1988)114:8(1804).

(73) Bosco, M., Ferrara, E., Ghersi, A., Marino, E.M., Rossi, P.P. (2016). Improvement of the model proposed by Menegotto and Pinto for steel. *Engineering Structures*, 124, 442-456. https://doi.org/10.1016/j.engstruct.2016.06.037.

(74) Spacone, E., Filippou, F. (1996, June). Flexibility-based frame models for nonlinear dynamic analysis. In Proceedings of the 11th World Conference on Earthquake Engineering, Acapulco, Mexico (pp. 23-28).

(75) Scott, M.H., Fenves, G.L., McKenna, F., Filippou, F.C. (2008). Software patterns for nonlinear beam-column models. *Journal of Structural Engineering*, 134(4), 562-571. https://doi.org/10.1061/(ASCE)0733-9445(2008)134:4(562).

(76) Crisafulli, F.J., Carr, A.J., Park, R. (2000). Analytical modelling of infilled frame structures. *Bulletin of the New Zealand society for earthquake engineering,* 33(1), 30-47. https://doi.org/10.5459/bnzsee.33.1.30-47.

(77) Crisafulli, F.J. (1997). Seismic behaviour of reinforced concrete structures with masonry infills. http://doi.org/10.26021/1979

(78) Calvi, G.M., Priestley, M.J.N., Kowalsky, M.J. (2007). Displacement based seismic design of structures. In New Zealand Conference on Earthquake Engineering (p. 740). IUSS press.

(79) Crisafulli, F.J., Carr, A.J. (2007). Proposed macro-model for the analysis of infilled frame structures. *Bulletin of the New Zealand society for earthquake engineering*, 40(2), 69-77. https://doi.org/10.5459/bnzsee.40.2.69-77

(80) Smyrou, E., Blandon, C., Antoniou, S., Pinho, R., Crisafulli, F. (2011). Implementation and verification of a masonry panel model for nonlinear dynamic analysis of infilled RC frames. *Bulletin of Earthquake Engineering*, 9(5), 1519-1534. https://doi.org/10.1007/s10518-011-9262-6.

(81) Antoniou, S., Pinho, R. (2004). Development and verification of a displacement-based adaptive pushover procedure. *Journal of Earthquake Engineering,* 8(05), 643-661. https://doi.org/10.1080/13632460409350504.

(82) Antoniou, S., Pinho, R. (2004). Advantages and limitations of adaptive and non-adaptive force-based pushover procedures. *Journal of Earthquake Engineering,* 8(04), 497-522. https://doi.org/10.1080/13632460409350498.

(83) Ferracuti, B., Pinho, R., Savoia, M., Francia, R. (2009). Verification of displacement-based adaptive pushover through multi-ground motion incremental dynamic analysis. *Engineering Structures*, 31(8), 1789-1799. https://doi.org/10.1016/j.engstruct.2009.02.035.

(84) Pinho, R., Bento, R., Bhatt, C. (2008, January). Assessing the 3D irregular spear building with nonlinear static procedures. In The 14th World Conference on Earthquake Engineering.

(85) Clough, R.W., Penzien, J. (1993). Dynamics of structures, MacGraw-Hill. Inc Editor. ISBN 0071132414, 9780071132411.
(86) Chopra, A.K. (1995). Dynamics of structures theory and. ISBN: 0-13-8552 4-2.
(87) FEMA 356, F. E. (2000). Prestandard and commentary for the seismic rehabilitation of buildings. Federal Emergency Management Agency, Washington, DC.
(88) ASCE. (2017). ASCE/SEI 41-17. Seismic evaluation and retrofit of existing buildings. Reston, VA, USA: ASCE.
(89) Stavridis, A., Martin, J., & Bose, S. (2017, September). Updating the ASCE 41 provisions for infilled RC frames. In Proceedings of the 2017 SEAOC Convention, San Diego, CA.
(90) Neuenhofer, A., Filippou, F.C. (1997). Evaluation of nonlinear frame finite-element models. Journal of structural engineering, 123(7), 958-966. https://doi.org/10.1061/(ASCE)0733-9445(1997)123:7(958).
(91) Park, Y.J., Ang, A.H.S. (1985). Mechanistic seismic damage model for reinforced concrete. Journal of structural engineering, 111(4), 722-739. https://doi.org/10.1061/(ASCE)0733-9445(1985)111:4(722).
(92) Huang, Z. M., & Chen, T. (2003). Comparison between flexibility-based and stiffness-based nonlinear beam-column elements (J). *Engineering Mechanics*, 5.
(93) Li, S; Zhai, C.H.; Xie, L.L. (2009). A review of flexibility-based finite element method for beam-column elements. *Journal of Harbin Institute of Technology*, 1.
(94) Alemdar, B.N., White, D.W. (2005). Displacement, flexibility, and mixed beam–column finite element formulations for distributed plasticity analysis. *Journal of Structural Engineering*, 131(12), 1811-1819. https://doi.org/10.1061/(ASCE)0733-9445(2005)131:12(1811).
(95) P.E. Mergos (2017). Optimum seismic design of reinforced concrete frames according to Eurocode 8 and fib Model Code 2010. *Earthquake Eng. Struct. Dyn.* 46(7), 1181–1201. https://doi.org/10.1002/eqe.2851.